Tolerance of platinum clusters to CO poisoning induced by molybdenum doping

Vladimir Kaydashev, Ewald Janssens, and Peter Lievens[*]

Laboratory of Solid-State Physics and Magnetism, KU Leuven, Celestijnenlaan 200d – box 2414, B-3001 Leuven, Belgium.

[*]Corresponding author: Peter Lievens, E-mail: peter.lievens@fys.kuleuven.be
Fax: +32 1632 7983; Tel: +32 1632 8498;
Vladimir Kaydashev, E-mail: kaydashev@gmail.com
Ewald Janssens, E-mail: ewald.janssens@fys.kuleuven.be

ABSTRACT

The influence of a single Mo dopant atom on the CO adsorption on isolated cationic platinum clusters in the gas phase, Pt_n^+ ($13 \leq n \leq 24$), has been investigated. The sticking probability of the first CO molecule to bare Pt_n^+ clusters is estimated to be close to unity and is not notably changed upon Mo doping. The adsorption probability of the second CO molecule, however, shows a significant reduction for $Pt_{n-1}Mo^+$ compared to Pt_n^+, reaching a maximal reduction of as much as 80% for $Pt_{19}Mo^+$. As a result, the average number of CO molecules adsorbed on Pt_n^+ with $19 \leq n \leq 24$, and surviving on the time scale of the experiment, decreases by about 10−15% upon substitution of a single Pt atom by a single Mo atom. A statistical analysis of the unimolecular dissociation of the cluster–CO complexes suggests that the lower sticking probability for the second CO molecule for Mo-doped species is related to a reduction of the CO chemisorption energy. Electron transfer from Mo to Pt resulting in a lowering of the Pt 5d vacancies and a downshift of the 5d-center is likely responsible for this reduced CO binding energy.

KEYWORDS: PtMo, doped platinum clusters, direct methanol fuel cell, unimolecular dissociation, CO tolerance

1. Introduction

In the last decades Pt and Pt alloys have been studied extensively as catalysts for proton exchange membrane fuel cells (PEMFCs).[1,2] CO poisoning of the platinum anode in these fuel cells is a serious problem and limits their performance. CO, being both a product of intermediate reactions and a pollutant in the fuel gas, blocks the active Pt catalytic sites.[3] The development of efficient catalysts requires inhibition of CO adsorption or the capability to oxidize adsorbed CO at low potentials. It has been demonstrated that certain Pt alloys, such as Pt-Ru, Pt-Mo, Pt-Nb, Pt-W, and Pt-Sn, have an improved CO tolerance.[4-8] In particular, the Pt-Mo alloy (4:1) shows an excellent long term stability and a threefold enhancement in CO tolerance with respect to the Pt-Ru alloy (1:1) at 100 ppm of CO in H_2.[4,9]

The mechanism of CO tolerance induced by alloying remains a subject of debate.[3,10-12] The anti-poisoning effect was first attributed to a bifunctional mechanism,[3] while the influence of an altered electronic structure upon alloying with a second metal, *Me*, was believed to be less important. According to the bifunctional mechanism, Pt catalyzing centers are released from CO groups via reactions between HCO or CO and HO groups situated on neighboring Pt and *Me* atoms, respectively.[3] Later on, several experimental[5,10,13] and theoretical[11,12,14] studies showed that electronic effects or ligand effects following alloying are also important. The CO electro-oxidation potential can be lowered by alloying because the Pt−CO bond strength decreases by modification of the electronic structure. Among the many Pt-*Me* nanostructures that have been studied, alloying with *Me* = Mo, W is theoretically predicted to result in a minimal CO binding energy.[14] Findings aimed to understand the details of CO tolerance are summarized in several reviews.[1,2,15,16]

Recent experiments on nanoparticles have shown that their catalytic activity increases faster with size reduction than the increase of the surface-to-volume ratio.[17] Composite materials based on atomic clusters are emerging as a promising class of novel functional materials for catalysis. The properties of clusters, consisting of a few tens of atoms, do not scale with their size, are extremely composition sensitive, and can be very different from the properties of their bulk counterparts. The addition of a single atom or a single electron can dramatically change the physical and chemical properties of metal clusters.[18,19,20] Fundamental research on clusters in the gas phase can be performed under well controlled conditions (fixed temperature, no contaminations, no influence of ambient or substrate) and is used to unravel fundamental

reaction mechanisms that are relevant for applied catalysis.[21] The CO chemisorption onto small Pt and some doped Pt clusters was studied experimentally[22,23] and theoretically.[24-28] Recently, the importance of electronic structure effects for CO tolerance enhancement was theoretically characterized for small Pt_nCu ($n \leq 7$) clusters and for alloy Pt-Ti clusters up to sizes of 201 atoms.[29,30] The effect of composition on the electronic structure in small clusters and the consequences for the CO adsorption energy have been illustrated for 13-atom Pt-Au clusters and demonstrated the importance of the local environment of the transition metal atom with the CO adsorbed.[31] The enhancement of the CO tolerance in comparison with bulk alloys was demonstrated for a number of Pt-*Me* (*Me* = Mo, Nb, Ru, Sn, and Ag) clusters and nanocrystals.[4,8,9,32-35] Related, a decrease of the CO adsorption energy on platinum monolayers deposited onto Mo(110), Nb(110) and W(110) were reported in early studies.[36-38]

In the present paper we characterize the influence of a single Mo dopant atom in small cationic platinum clusters on the adsorption of CO molecules. The adsorption probability of one and two CO molecules on bare Pt_n^+ and molybdenum doped $Pt_{n-1}Mo^+$ ($13 \leq n \leq 24$) clusters is studied in the gas phase at room temperature. The simultaneous measurement of the reactivity of bare and doped clusters allow to quantify the influence of the dopant atom on the adsorption probability. The well defined conditions in a gas phase experiment allow to exclude the presence of other functional groups (such as OH) and bifunctional mechanisms can thus not take place. The observed enhanced CO tolerance upon Mo doping is therefore solely related to changes in the electronic structure. Although conditions far from those in real fuel cells are used, the results provide relevant fundamental information about phenomena that occur in real devices.

2. Experimental

The bare platinum and molybdenum doped platinum cluster cations, Pt_n^+ and $Pt_{n-1}Mo^+$, are produced by ablation of Pt and Mo targets (99.95% purity) in a laser vaporization source operated at room temperature.[39] The amount of ablated material is controlled by two independent pulsed Nd:YAG lasers (532.8 nm, 10 Hz) with pulse energies of about 50 mJ and 90 mJ for Pt and Mo, respectively. The He gas (backing pressure 8 bar) is introduced by a pulsed (10 Hz) supersonic valve just before laser ablation of the targets. The clusters are thermalized by heat exchange with walls of the source via collisions with He carrier gas and adiabatically expand into vacuum resulting in a molecular beam of clusters. It is assumed that the temperature of the

clusters equals the temperature of the source (i.e., 300K). The validity of this assumption was confirmed in earlier work where argon absorption was studied as function of the source temperature.[40]

The central part of the cluster beam is selected by a conical skimmer. The cluster size distribution is analyzed by a reflectron time-of-flight mass spectrometer with mass resolution $M/\Delta M = 600$. The attachment of CO molecules to the clusters is studied using a low pressure collision cell, which has been discussed in detail elsewhere.[18] The introduction of CO gas in the reaction cell is controlled by a needle valve. The pressure in the cell is monitored by a capacitance gauge (Varian CMH4) and was maintained in the range of $1-6\times10^{-2}$ Pa. The experiments are carried out at room temperature. Under these conditions, cluster−CO complexes, $[Pt_n\cdot(CO)_m]^+$ and $[Pt_{n-1}Mo\cdot(CO)_m]^+$, with $m \leq 2$ for $n \leq 24$ are observed. For CO pressures larger than 6×10^{-2} Pa, $m = 3$ complexes are formed and there is a significant overlap of species in the mass spectra.

3. Results and discussion

3.1 Data evaluation

A typical mass spectrum of Pt_n^+ and $Pt_{n-1}Mo^+$ ($18 \leq n \leq 22$) clusters that have reacted with CO in the low pressure collision cell is shown in Fig. 1. From comparison of bare platinum and molybdenum doped platinum mass spectra, we are confident that no (or very few) $Pt_nMo_m^+$ with $m \geq 2$ clusters are produced under these experimental conditions. However, small traces of atomic oxygen on both Pt_n^+ and $Pt_{n-1}Mo^+$, stemming from the Mo target and impurities in the carrier gas, are detectable for the smallest investigated cluster sizes. The contamination is lower for larger clusters and shows up as small, hardly noticeable, shoulders. In the reactivity analysis the abundances were corrected for the presence of these contaminants.

At a pressure as low as 5×10^{-2} Pa, corresponding to an average of about 0.75 collisions experienced by each cluster passing through the cell, clusters with $n = 13-24$ readily form CO complexes. Pt_n^+ and $Pt_{n-1}Mo^+$, with $n = 16-24$, also form a significant fraction of $(CO)_2$ complexes. As can be seen in Fig. 1 the intensity ratios of $[Pt_n\cdot CO]^+$ to Pt_n^+ and of $[Pt_{n-1}Mo\cdot CO]^+$ to $Pt_{n-1}Mo^+$ are comparable, while the intensity ratio of $[Pt_n\cdot(CO)_2]^+$ to Pt_n^+ is higher than that of $[Pt_{n-1}Mo\cdot(CO)_2]^+$ to $Pt_{n-1}Mo^+$ for $18 \leq n \leq 22$. Especially $Pt_{19}Mo^+$ and $Pt_{20}Mo^+$ show a local

minimum for $(CO)_2$ adsorption. These mass spectrometric observations are the basis for the later conclusions of the current study.

Passing through the collision cell at a certain CO pressure P_{CO}, a cluster experiences an average number of collisions, N, that can be approximated using hard sphere collision theory:

$$N = \sigma L_{cell} \frac{P_{CO}}{k_B T_{CO}} \frac{v_{relative}}{v_{cluster}} \quad (1)$$

where L_{cell} = 6 cm is the length of the collision cell, T_{CO} is the CO gas temperature in the reaction cell which is assumed to be 300 K, and k_B is the Boltzman constant. $v_{relative}/v_{cluster}$ is the ratio of the average relative cluster−CO velocity to the absolute velocity of the cluster and is equal to 1.08 at 300 K. The direction of the velocity of the CO molecules is random and their speed can be modeled by a Boltzmann distribution. The $v_{relative}/v_{cluster}$ ratio was derived by averaging the direction and magnitude distribution of the velocity of the CO molecules, relative to the fixed velocity (~1100 m/s) of the clusters. The collision cross section σ can be approximated by a hard-sphere model:

$$\sigma = \pi(R_{CO} + R_n)^2 \quad (2)$$

A cluster consisting of n atoms is assumed to have a radius $R_n = n^{1/3} r_b + d$ and the same density as the bulk (atomic radius of Pt r_b=1.387 Å).[41] The constant d accounts for the deviation from a perfect spherical shape. A typical value of 0.5 Å was used. R_{CO}, representing the radius of a CO molecule, was set to 1.9 Å. This geometrical model for Pt_n^+ is a rough approximation, since the real structure of these clusters are not expected to be perfect spheres. For neutral Pt_n in the range n = 10–20 layered and pyramidal structures are predicted, while decahedral isomers are favorable for n = 21–24.[27,42] A systematic uncertainty could originate from an over- or underestimation of bond lengths (periodic lattice in bulk versus bond distances in small clusters), while a statistical uncertainty could be related to size-to-size variations in the geometric structure of the clusters, which are ignored in the spherical approximation. The statistical uncertainty can be approximated by variations of the cross sections for different Pt_n isomers at given size n, which is about 10%.[27] As a result size-to-size or dopant induced variations of the CO sticking probability up to 10% could originate from size-to-size or dopant induced deviations of the actual cross section relative to the assumed cross section using a spherical geometry. As we will

show below, larger changes of the CO sticking probabilities following Mo doping are found in the current study, which will be attributed to CO binding energy changes.

In bulk Pt-Mo (1:3) alloys the Pt−Mo bond lengths are ~2.756 Å, which is close to the Pt−Pt bond length in fcc platinum.[43] Therefore, the radii of $Pt_{n-1}Mo^+$ clusters can be assumed to be similar to those of Pt_n^+.

The reactivity measurements were performed in the CO pressure range of $1-6\times10^{-2}$ Pa, corresponding to average ranges of 0.15−0.90 collisions for Pt_{13} to 0.19−1.15 collisions for Pt_{24}. Since the number of collisions follows a Poisson distribution, an average number of collisions equal to 0.5 implies that about 60% of the clusters have no collisions, 30% one collision, 8% two collisions, and 1% three or more collisions.

No $Pt_{n,n-1}Mo_{0,1}^+\cdot(CO)_k$ ($k > 2$) species were observed under the applied pressure and temperature conditions; the probability of the formation of complexes with 3 CO molecules is therefore assumed to be zero. The simplest reaction mechanism, considering only CO attachment, is thus:

$$\begin{aligned} Pt_{n,n-1}Mo_{0,1}^+ + CO &\xrightarrow{S_1} \left[Pt_{n,n-1}Mo_{0,1}\cdot(CO)\right]^+ \\ \left[Pt_{n,n-1}Mo_{0,1}\cdot(CO)\right]^+ + CO &\xrightarrow{S_2} \left[Pt_{n,n-1}Mo_{0,1}\cdot(CO)_2\right]^+ \end{aligned} \qquad (3)$$

Here, S_1 and S_2 are probabilities for successful adsorption, or sticking probability, of one and two CO molecules onto a cluster, respectively. These sticking probabilities S_1 and S_2 reflect the probability that cluster−$(CO)_{1,2}$ complexes are formed in the reaction cell and survive until detection. The attachment reactions of Eq. (3) are actually the net result of association and desorption reaction steps. Indeed, CO desorption (or statistical cluster−$(CO)_{1,2}$ dissociation) can take place when the internal energy is higher than the desorption barrier. Formally both association (4a) and dissociation (4b) reaction steps should be considered inside the reaction cell, while outside the cell only dissociation (4b) is possible: [18]

$$Pt_{n,n-1}Mo_{0,1}^+ + CO \xrightarrow{k_f} \left[Pt_{n,n-1}Mo_{0,1}\cdot(CO)\right]^+ \qquad (4a)$$

$$\left[Pt_{n,n-1}Mo_{0,1}\cdot(CO)\right]^+ \xrightarrow{k_d} Pt_{n,n-1}Mo_{0,1}^+ + CO \qquad (4b)$$

Here, k_f is the bimolecular rate coefficient for formation of cluster−CO complexes and k_d is the unimolecular dissociation rate coefficient. Mechanisms taking into account the back reaction within and outside the collision cell did not improve the description of the data, probably because of the low pressure range used in this experiment corresponding to less than one collision per cluster on average and we therefore continue with the overall mechanism described in Eq. 3. The role of the back reaction will however be detailed further in section 3.2.

The reactions of Eq. (3) are first order with respect to the reactants. Since there is a continuous flow of CO gas in the reaction cell and only a negligible fraction of it is consumed, there is an excess of CO gas. Consequently, the pseudo-first-order conditions are satisfied for the overall reaction and the intensities of the bare clusters, I_0, and of the cluster−$(CO)_k$ complexes, I_k (k = 1,2), should vary with N, the average number of collisions as:

$$\begin{cases} \dfrac{dI_0}{dN} = -I_0 S_1 \\ \dfrac{dI_1}{dN} = I_0 S_1 - I_1 S_2 \\ \dfrac{dI_2}{dN} = I_1 S_2 \end{cases} \Leftrightarrow \begin{cases} I_0 = I_i \exp(-S_1 N) \\ I_1 = I_i \dfrac{S_1}{S_1 - S_2} (\exp(-S_2 N) - \exp(-S_1 N)) \\ I_2 = 1 - I_0 - I_1 \end{cases} , \qquad (5)$$

with I_i the intensity of the bare cluster before passing through the low pressure collision cell.
The measured intensities, I_k, may slightly differ from the corresponding intensities at the end of the reaction cell because the clusters are scattered by collisions with the CO molecules. This may cause deflection of clusters out of the collimated molecular beam and, thus, out of the detection region.[19,20] However, since the fraction of deflected clusters is below 5% at the maximal applied pressure and deflection affects both the intensities of the reacted and the bare clusters (after backward reaction), and has less influence on their ratio, no correction was made for this.

A typical example of the dependence of the relative abundances, I_k/I_i (k = 0−2), on N is illustrated in Fig. 2 for Pt_{20}^+ and $Pt_{19}Mo^+$. Fitting of the experimental values by the pseudo first order kinetics model (5), provides the CO sticking probabilities S_1 and S_2.

The derived S_1 and S_2 values are given in Fig. 3. The error bars represent the uncertainties that result from the fitting combined with a 10% uncertainty on the average number of collisions, N. The sticking probabilities of the first CO molecule on bare Pt_n^+ are nearly constant and close to unity in the considered size range, n = 13−24, while S_2 demonstrates a monotonic growth with

cluster size in addition to an even-odd oscillation for n = 18−22 (Fig. 3a). Cluster cations Pt_n^+ with even n have a slightly lower CO adsorption probability. Considering an itinerant electron model for atomic clusters such oscillation is usually associated with filling of electronic sub-shells.[19] Upon Mo doping the sticking probability for the first CO molecule, S_1, does not notably change and remains close to unity. Meanwhile the adsorption probability of the second CO molecule, S_2, is significantly reduced for the Mo doped clusters (Fig. 3a).

3.2 Presence of a back reaction

The reaction mechanism described by Eq (3) is the simplest mechanism that agrees with the experimental data. However, unimolecular dissociation of the cluster−CO complexes, Eq (4b), can take place as mentioned above. More complex processes, e.g., cluster fragmentation via the loss of a Pt atom, did not improve the fit quality. Pt evaporation following on the CO adsorption is unlikely because the cohesive energy per Pt atom in a Pt_n cluster is higher than the CO adsorption energy. Typical Pt binding energies in Pt_n clusters are 2.65 eV for $n = 10$[44] and 3.5–3.88 eV for n = 6–10,[45] while calculated CO adsorption energies on Pt_n clusters are 2.21–2.73 eV for Pt_6,[24] 2.30–2.36 eV (for atop site) and 1.49–1.95 eV (for bridge site) for Pt_{10}.[41] The absence of the fragmentation channel upon CO adsorption was also found previously for anions.[46]

In the current experiments CO desorption takes place as is reflected by the increase of S_2 with cluster size, which in turn is related to the limited possibility to accommodate the heat of formation in small clusters.[18] The number of degrees of freedom, among which the energy can be distributed, increases with increasing cluster size. Thus, for a fixed CO chemisorption energy, the survival time of the cluster−molecule complex increases with cluster size. The survival time (which is the inverse of the unimolecular dissociation rate, k_d) is directly related to the sticking probability. The sticking probability is in essence a combination of CO absorption and survival of the cluster−CO complex on the time scale of the experiment ($t \approx 100$ μs). Roughly stated $S \approx \exp(-k_d t)$, which means that $S \approx 1$ (values found experimentally for S_1) implies $k_d << 10^4$ s^{-1}, and the range of S = 0.1–0.5 (values found for S_2 in the n = 17–23 size range) corresponds to $k_d = 2\times10^4$–7×10^3 s^{-1}.

3.3 Statistical modelling of the reaction

The rate of the back reaction, and thus of the experimentally derived $S_{1,2}$ values, is related to the $(CO)_{1,2}$ binding energies. To illustrate the dependence of k_d on the CO chemisorption energy, E_b, a statistical RRKM analysis is carried out.

Unimolecular dissociation rates of the cluster−CO complexes are calculated using the *MassKinetics* software package.[47] As input for the RRKM analysis, the frequencies of the Pt clusters are approximated by a discrete Debye model.[48] The translational energy of the cluster was not included in the analysis, since the speed of the clusters remains basically unchanged after collision with the CO gas and is thus not available for the backward reaction. When modelling the detachment of the second CO molecule it was assumed that the first CO was bound by 2.75 eV.

This value is taken from a theoretical calculation of the CO chemisorption energies on Pt clusters, which gave values of 2.73 eV and 2.21 eV for the first and second CO molecule on Pt_6, respectively.[24] If k_d is lower than $1x10^4$ s^{-1}, the complexes are (on average) stable at the time scale of the experiment. While this simple model does not capture any details of the electronic and geometric structure, it reflects the role of the cluster size to accommodate the released heat upon complex formation.

As an example Fig. 4 shows the dependence of k_d on the CO chemisorption energy for $Pt_{13}{\cdot}(CO)_k$ and $Pt_{18}{\cdot}(CO)_k$ with k = 1, 2. It can be seen that for a given E_b the larger cluster has a lower k_d (or a longer lifetime). It can also be observed that the survival times of the cluster–$(CO)_2$ complexes are lower than those of the clusters that absorbed only one CO molecule. This is because those clusters are already heated up by the absorption of the first CO. The numerical values hint that our experimental approach is sensitive to binding energy changes for the $(CO)_2$ complexes since these are predicted to have k_d values in the range corresponding to the time scale of the experiment (horizontal dotted line in Fig. 4), while the experimental approach likely is not sensitive to small changes in the binding energy of the first CO molecule.

3.4 CO tolerance induced by doping

The results of the RRKM analysis facilitate the interpretation of the experimental data. We indeed observed a strong size and dopant dependence for S_2 but not for S_1 (Fig. 3a). This reflects

the fact that the survival times of the $[Pt_{n,n-1}Mo_{0,1}\cdot(CO)_2]^+$ and $[Pt_{n,n-1}Mo_{0,1}\cdot(CO)]^+$ complexes are comparable to and longer than the time scale of the experiment, respectively. S_1 is about 0.9−1.0 for $n \geq 13$, which is in good agreement with the value of 0.85, measured by Campbell *et al.* for a bulk Pt(111) surface at room temperature.[46] Also the current experiments are done with the cluster source at room temperature. But quantitative comparison of the temperature dependent sticking probabilities should be done with care since the exact temperature of the clusters depends the degree of thermalization, which is sensitive to source parameters such as ablation laser fluence and the geometry of the nozzle.

Because the heat of formation should be accommodated in the cluster−CO complex, the sticking probability decreases with increasing cluster temperature.[20] It should be noted that after the adsorption of the first CO molecule the temperature of different cluster sizes may be slightly different. Comparing the pure and Mo doped platinum clusters, the Mo doped clusters are expected to be slightly colder after attachment of the first CO molecule because of likely reduction in the binding energy upon doping.[13]

Since the Pt_n^+ and $Pt_{n-1}Mo^+$ clusters are produced under the same source conditions (except for the above remark on the temperature after the absorption of the first CO molecule), the changes of S_1 and S_2 upon doping allow to qualitatively characterize the effect of Mo doping on CO tolerance of platinum clusters. In particular, the decrease of S_2 upon doping the Pt_n^+ cluster with Mo (Fig. 3a), is a reflection of the reduced CO chemisorption energy, E_b.

The average number of CO molecules absorbed on a given cluster size is calculated from the integrated abundances as

$$M_{\mathrm{CO}}(X_n) = \left[I_{X_n\cdot\mathrm{CO}} + 2I_{X_n\cdot(\mathrm{CO})_2}\right] \Big/ \left[I_{X_n} + I_{X_n\cdot\mathrm{CO}} + I_{X_n\cdot(\mathrm{CO})_2}\right], \qquad (6)$$

and plotted in Fig. 3b. M_{CO} decreases by 10−15% for $19 \leq n \leq 24$ upon substitution of a platinum atom by a molybdenum atom. A local minimum of CO adsorption is observed for $Pt_{19}Mo^+$. The strong size dependence of the influence of the dopant atom on size is illustrated in Fig. 3c that shows the ratio of S_2 values of Mo-doped vs. pure Pt clusters. In particular, S_2 of $Pt_{19}Mo^+$ is 80% than that of Pt_{20}^+. For Pt_n^+ clusters with $13 \leq n \leq 16$ no significant change of the CO adsorption probability following Mo doping is observed.

The CO chemisorption on Pt is traditionally described by the Blyholder model. The bonding is a combination of electron donation from the 5σ-orbital of CO to the 5d-band of Pt, and back

donation of 5d electrons of Pt to the two π* antibonding orbitals of CO.[9,50,51] Ray and Anderson[52] have found that the effect of 5σ-orbital stabilization of CO is the main factor responsible for the bond strength with the amount of charge transfer from the CO 5σ-orbital to the Pt 5d-band playing a major role. It was also found that the charge redistribution upon doping nanoparticles may be accompanied by a shift of the center of the Pt 5d-band position, which is the most decisive parameter for the CO chemisorption energy.[30] More general, it has been shown that the center of the d-band relative to the Fermi energy plays a key role in the reactivity of transition metals in different environments with increasing adsorption energies as the d-band center shifts to higher energies.[52] In few-atom clusters, the molecular orbitals are energetically separated and no bands are formed. Conceptually, however, similar dopant induced changes of the electronic structures are predicted. In particular, the adsorption energy of CO on a Pt site in 13-atom Pt-Au clusters was shown to decrease with the Au content in the cluster.[31] The local environment of the adsorption site (preferentially a Pt atom) determines the properties of the Pt–CO bond. Upon alloying the Pt_{13} clusters with Au, the d-center, which is calculated as the first moment of the density of states of the projected d-orbitals with respect to the Fermi level at the adsorption site, shifts to lower energies resulting in a lower CO adsorption energy.

Analogous conclusions were obtained in a theoretical study of 201-atom Pt-Ti alloy clusters: electron donation from Ti to the Pt d-orbitals downshifts in Pt 5d-center, with weaker CO binding as a consequence.[30] In larger Pt-Mo (~3−4 nm)[12] and Pt-Au (~1.5−3 nm)[54] alloy particles an electron transfer from Mo/Au to Pt associated with a decrease of electron vacancies in the atomic Pt 5d levels and a lowering of the Pt 5d-center is consistent with experimental XANES spectra where a decrease of the LIII – edge peak was found in comparison with pure Pt particles.

Our experiments (Fig. 3b) show that the CO abundance per Pt_n^+ cluster is remarkably decreased (10-15%, depending on size) in the $19 \leq n \leq 24$ size range upon substitution of a single platinum atom by a molybdenum atom, whereas for sizes $13 \leq n \leq 16$ there is no significant change. We speculate that the larger Pt_n^+ clusters may have a caged structure accommodating the Mo atom. The encapsulated Mo atom could more effectively change Pt−Mo and Pt−Pt interatomic distances and enhance hybridization of electronic orbitals, making the charge transfer easier. There exist theoretical predictions of an empty caged structure for Pt_{22},[23] but doped platinum clusters with more than 13 atoms still remain poorly studied.

As the theoretical studies about the local molecular orbital overlap and binding energies at

different adsorption sites are not available in literature neither for bare Pt_n^+ nor for doped $Pt_{n-1}Mo^+$ clusters, only a conceptual interpretation of the data can be given. In particular, at small pressures the CO is preferably adsorbed onto Pt_n^+ clusters by binding the carbon atom in atop-sites.[22] Earlier temperature programmed CO desorption measurements onto thin film Pt/Mo(110) showed that the Mo atom can decrease the CO−Pt binding energy only for 1-2 monolayers of Pt.[36] Similarly, the decrease of the CO adsorption energy on Pt atoms in the $Pt_{n-1}Mo^+$ clusters is expected to depend on the Mo coordination number.

4. Conclusions

We have investigated the influence of a single Mo dopant atom on the tolerance of small platinum clusters Pt_n^+ ($13 \leq n \leq 24$) towards CO poisoning using a low pressure collision cell. While for the smaller sizes studied, Pt_n^+ with $13 \leq n \leq 18$, no significant change in the CO tolerance was observed, the average number of absorbed CO molecules on the larger ($19 \leq n \leq 24$) clusters decreased by 10−15% upon the substitution of a single platinum atom by a single molybdenum atom. The sticking probability for the first CO molecule S_1 did not notably change upon doping and is close to unity under the current experimental conditions. Meanwhile the adsorption probability of the second CO molecule S_2 is significantly reduced upon doping, with a maximal decrease of the relative sticking probability of 80% for $Pt_{19}Mo^+$. RRKM analysis showed that this reduction is a reflection of a reduction of the CO chemisorption energy upon doping the clusters.

Our experiments suggest that the reduction of CO adsorption energies is due to dopant induced changes of the local electronic structure at the Pt absorption site. The alternative explanation that dopant induced structural changes cause a reduction of the CO binding energy is unlikely because the tolerance is observed over a large size range. Such dopant induced reduction of the CO chemisorption energy is an important factor to improve the CO tolerance of Pt_n catalysts. As even single atom doping remarkably changes the tolerance, it can be expected that increasing the Mo content in the Pt_n clusters could lead to a further enhancement of CO tolerance.

Under the current experimental conditions, bifunctional mechanisms where the Pt catalyzing centers are released from CO groups via reactions between HCO or CO and HO groups situated on neighboring Pt and dopant atoms, are not possible. The small traces of oxygen atoms detected in our experiment are much smaller than concentrations of adsorbed CO. However, in real

PEMFC conditions one could expect that cluster-based Pt-Mo catalysts should follow a bifunctional mechanism to clean the Pt. Indeed, although reduced, the doped clusters still show CO adsorption and a supplementary mechanism is required to get rid of the CO.

We hope that the present experimental results will inspire further computational studies on dopant induced changes of the electronic structure of small platinum clusters.

Acknowledgments

This work is supported by the Research Foundation - Flanders (FWO), by the KU Leuven Research Council (BOF, GOA, and IDO programs), and by the COST Action MP0903 "Nanoalloy".

References

[1] S. Ye, in: J. J. Zhang (Ed.), PEM Fuel Cell Electrocatalysts and Catalyst Layers: Fundamentals and Applications, Springer, London, 2008, pp.759-811.

[2] X. Zhao, M. Yin, L. Ma, L. Liang, C. Liu, J. Liao, T. Lu and W. Xing, Energy Environ. Sci., 2011, **4**, 2736.

[3] M. Watanabe, and S. Motoo, Electrtoanal. Chem. Int. Electrochem., 1975, **60**, 267.

[4] B. N. Grgur, N. M. Markovic, P. N. Ross, J Electrochem. Soc., 1999, **146**, 1613.

[5] J. McBreen and S. Mukerjee, J. Electrochem. Soc., 1995, **142**, 3399.

[6] W. J. Zhou, B. Zhou, W. Z. Li, Z. H. Zhou, S. Q. Song, G. Q. Sun, Q. Xin, S. Douvartzides, M. Goula, P. Tsiakaras, J. Power Sources., 2004, **126**, 16.

[7] M. Götz and H. Wendt, Electrochimica Acta. 1998, **43**, 363.

[8] T. A. Rocha, F. Ibanhi, F. Colmati, J. J. Linares, V. A. Paganin, E. R. Gonzalez, J. Appl. Electrochem., 2013, **43**, 817.

[9] S. Mukerjee, R.C. Urian, S. J. Lee, E. A. Ticianelli, J. McBreen, J. Electrochem. Soc., 2004, **151**, A1094.

[10] H. Igarashi, T. Fujino, Y. Zhu, H. Uchida and M. Watanabe, Phys. Chem. Chem. Phys., 2001, **3**, 306.

[11] P. Liu, J. K. Nørskov, Fuel Cells., 2001, **1**, 192.

[12] E. Christoffersen, P. Liu, A. Ruban, H. L. Skriver, and J. K. Nørskov, J. Catal., 2001, **199**, 123.

[13] J. H. Bang and H. Kim, Bull. Korean Chem. Soc., 2011, **32**, 3660.

[14] Y. Ishikawa, M. S. Liao, C. R. Cabrera, Surf. Sci., 2002, **513**, 98.

[15] R. C. Urian, A. F. Gulla, S. Mukerjee, J. Electroanal. Chem., 2003, **554**, 307.

[16] J. H. Wee, K. Y. Lee, J. Power Sources., 2005, **157**, 128.

[17] K. Yamamoto, T. Imaoka, W. J. Chun, O. Enoki, H. Katoh, M. Takenaga and A. Sonoi, Nat. Chem., 2009, **1**, 397.

[18] H. T. Le, S. M. Lang, J. De Haeck, P. Lievens, and E. Janssens, Phys. Chem. Chem. Phys., 2012, **14**, 9350.

[19] N. Veldeman, P. Lievens, and M. Andersson, J. Phys. Chem. A., 2005, **109**, 11793.

[20] J. De Haeck, N. Veldeman, P. Claes, E. Janssens, M. Andersson, and P. Lievens J. Phys. Chem. A., 2011, **115**, 2103.

[21] D. K. Böhme and H. Schwarz, Angew. Chem. Int. Ed., 2005, **44**, 2336.

[22] P. Gruene, A. Fielicke, G. Meijer and D. Rayner, Phys. Chem. Chem. Phys., 2008, **10**, 6144.

[23] G. Ganteför, G. Schulze Icking-Konert, H. Handschuh, W. Eberhardt, Int. J. Mass Spectrom. Ion Processes, 1996, **159**, 81.

[24] L. Chen, B. Chen, C. Zhou J. Wu, R. C. Forrey, H. Cheng, J. Phys. Chem. C., 2008, **112**, 13937.

[25] Y. Shimodaira, T. Tanaka, T. Miura, A. Kudo, and H. Kobayashi, J. Phys. Chem. C., 2007, **111**, 272.

[26] M. S. Liao, C. R. Cabrera, Y. Ishikawa, Surf. Sci., 2000, **445**, 267.

[27] V. Kumar, and Y. Kawazoe, Phys. Rev. B, 2008, **77**, 205418.

[28] L. Li, A. H. Larsen, N. A. Romero, V. A. Morozov, C. Glinsvad, F. A. Pedersen, J. Greeley, K. W. Jacobsen, and J. K. Nørskov, J. Phys. Chem. Lett., 2013, **4**, 222.

[29] X. L. Lei, M. S. Wu, G. Liu, B. Xu, and C. Y. Ouyang, J. Phys. Chem. A., 2013, **117**, 8293.

[30] P. C. Jennings, B. G. Pollet, and R. Johnston, J. Phys. Chem. C., 2012, **116**, 15241.

[31] B. H. Morrow, D. E. Resasco, A. Striolo, M. B. Nardelli, J. Phys. Chem. C, 2011, **115**, 5637.

[32] Y. Y. Feng, L. X. Bi, Z. H. Liu, D. S. Kong, Z. Y. Yu, J. Catal., 2012, **290**, 18.

[33] J. H. Kim, S. M. Choi, S. H. Nam, M. H. Seo, S. H. Choi and W. B. Kim, Appl. Catal. B., 2008, **82**, 89.

[34] T. Yamanaka, T. Takeguchi, G. Wang, E. N. Muhamad, W. Ueda, J. Power Sources., 2010, **195**, 6398.

[35] J. E. Hu, Z. Liu, B. W. Eichhorn, G. S. Jackson, Int. J. Hydrogen Energy., 2012, **37**, 11268.

[36] A. Linsebigler, G. Lu and J. Yates, Surf. Sci., 1993, **294**, 284

[37] X. Pan, M. W. Ruckman, M. Strongin, Phys. Rev. B, 1987, **35**, 3734

[38] R. A. Demmin, S. M. Shivaprasad, T. E. Madey, Langmuir, 1988, **4**, 1104

[39] W. Bouwen, P. Thoen, F. Vanhoutte, S. Bouckaert, F. Despa, H. Weidele, R. Silverans, and P. Lievens, Rev. Sci. Instrum., 2000, **71**, 54.

[40] E. Janssens, P. Gruene, G. Meijer, L. Wöste, P. Lievens, and A. Fielicke, Phys. Rev. Lett. , 2007, **99**, 063401.

[41] J. W. Arblaster, Platinum Mater. Rev., 1997, **41**, 1.

[42] L. Xiao and L. Wang, J. Phys. Chem. A, 2004, **108**, 8605.

[43] A. A. Knizhnik, A. V.Gavrikov, A. A.Safonov, I. M. Iskandarova, A. A. Bagatur`yants, B. V. Potapkin, L. R. C. Fonseca, M. W. Stoker, J. Appl. Phys., 2006, **100**, 013506.

[44] R. M. Watwe, B. E. Spiewak R. D. Cortright and J. A. Dumesic, Catal. Lett., 1998, **51**, 139.

[45] J. Kua and W. A. Goddard, J. Phys. Chem. B, 1998, **102**, 9481 .

[46] K. M. Ervin, Int . Rev. Phys. Chem., 2001, **20**, 127.

[47] L. Drahos, K. Vekey, J. Mass Spectrom., 2001, **36**, 237.

[48] A. A. Shvartsburg, K. M. Ervin, and J. H. Frederick, J. Chem. Phys., 1996, **104**, 8458.

[49] C. T. Campbell, G. Ertl, H. Kuipers, and J. Segner, Surf. Sci., 1981, **107**, 207.

[50] G. J. Blyholder, J. Phys. Chem., 1964, **68**, 2772.

[51] B. Hammer, Y. Morikawa, J. K. Nørskov, Phys. Rev. Lett., 1996, **76**, 2141.

[52] N. K. Ray, A. B. Anderson, Surf. Sci., 1982, **119**, 35.

[53] J. R. Kitchin, J. K. Nørskov, M. A. Barteau, J. G. Chen, J. Chem. Phys., 2004, **120**, 10240.

[54] E. Bus and J. A. van Bokhoven, J. Phys. Chem. C., 2007, **111**, 9761.

Fig. 1 Mass spectrum of Pt_n^+ and $Pt_{n-1}Mo^+$ ($18 \leq n \leq 22$) clusters that have reacted with CO in the low pressure collision cell at a CO pressure of 5×10^{-2} Pa. Signal is colored to visualize differences in intensity ratios of reacted to unreacted clusters upon Mo doping: Pt_n^+ (light blue), $[Pt_n\cdot CO]^+$ (dark blue), $[Pt_n\cdot(CO)_2]^+$ (orange), $Pt_{n-1}Mo^+$ (green), $[Pt_{n-1}Mo\cdot CO]^+$ (yellow), and $[Pt_{n-1}Mo\cdot(CO)_2]^+$ (red).

Fig. 2 Relative abundances of Pt_{20}^+ and $Pt_{19}Mo^+$ clusters and their CO complexes as function of the average number of collisions between the clusters and CO. The lines are fits using Eq. (4).

Fig. 3 Absorption probability for the first (S_1) and second (S_2) CO molecule on Pt_n^+ and $Pt_{n-1}Mo^+$ clusters (a). Average number of CO molecules absorbed on the clusters (M_{CO}) as function of the cluster size for a CO pressure of 6×10^{-2} Pa (b). The ratios of CO adsorption probabilities onto bare and Mo doped platinum clusters S_n(doped)/S_n(bare), n=1,2 (c).

Fig. 4 Dependence of the unimolecular dissociation rate, k_d, of $Pt_{13}\cdot(CO)_k$ and $Pt_{18}\cdot(CO)_k$ for k = 1, 2 on the CO chemisorption energy employing RRKM theory. For k = 2 the chemisorption energy of the first CO molecule was assumed to be E_b = 2.75 eV. k_d values smaller than 10^4 s^{-1} (indicated by the horizontal dotted line) imply that most cluster−CO complexes survive on the time scale of the experiment.

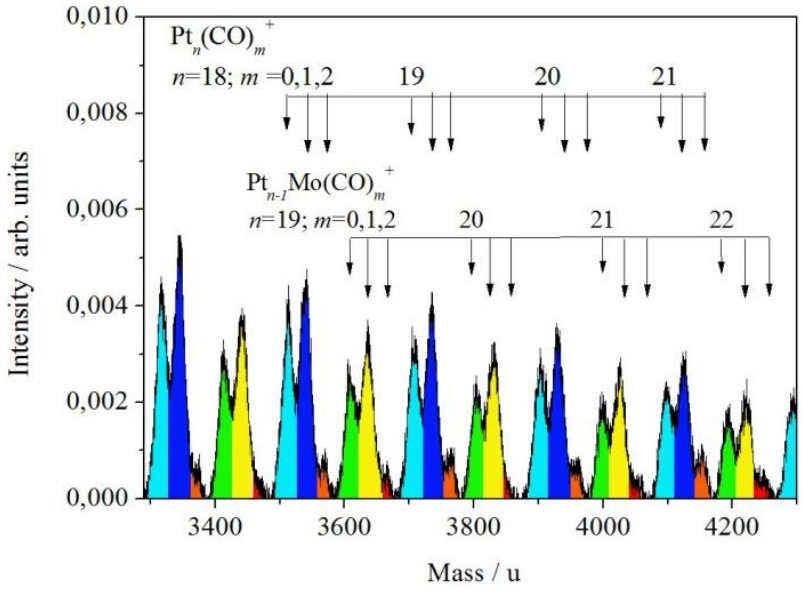
0,010
0,008
0,006
0,004
0,002
0,000
Intensity / arb. units
$Pt_n(CO)_m^+$
n=18; m =0,1,2
19
20
21
$Pt_{n-1}Mo(CO)_m^+$
n=19; m=0,1,2
20
21
22
3400
3600
3800
4000
4200
Mass / u

Fig. 1

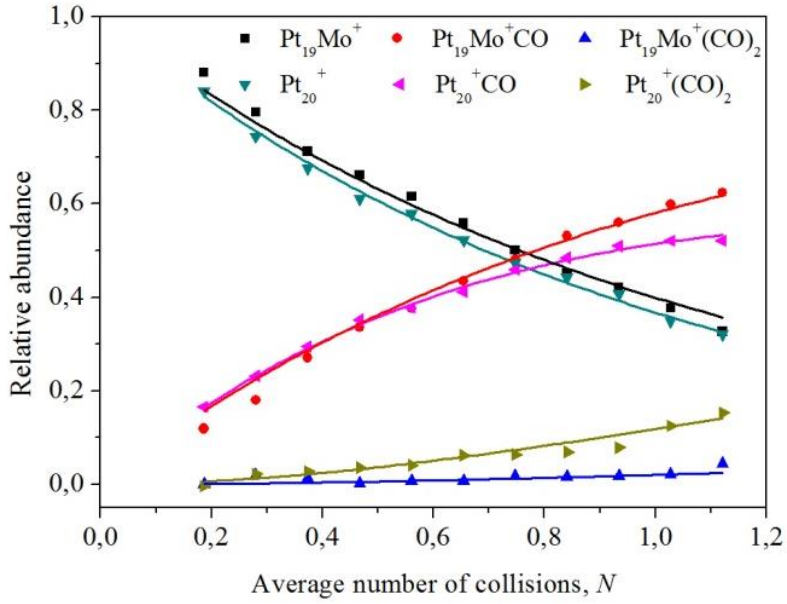
1,0
0,8
0,6
0,4
0,2
0,0
Relative abundance
$Pt_{19}Mo^+$
$Pt_{19}Mo^+CO$
$Pt_{19}Mo^+(CO)_2$
Pt_{20}^+
Pt_{20}^+CO
$Pt_{20}^+(CO)_2$
0,0
0,2
0,4
0,6
0,8
1,0
1,2
Average number of collisions, N

Fig. 2

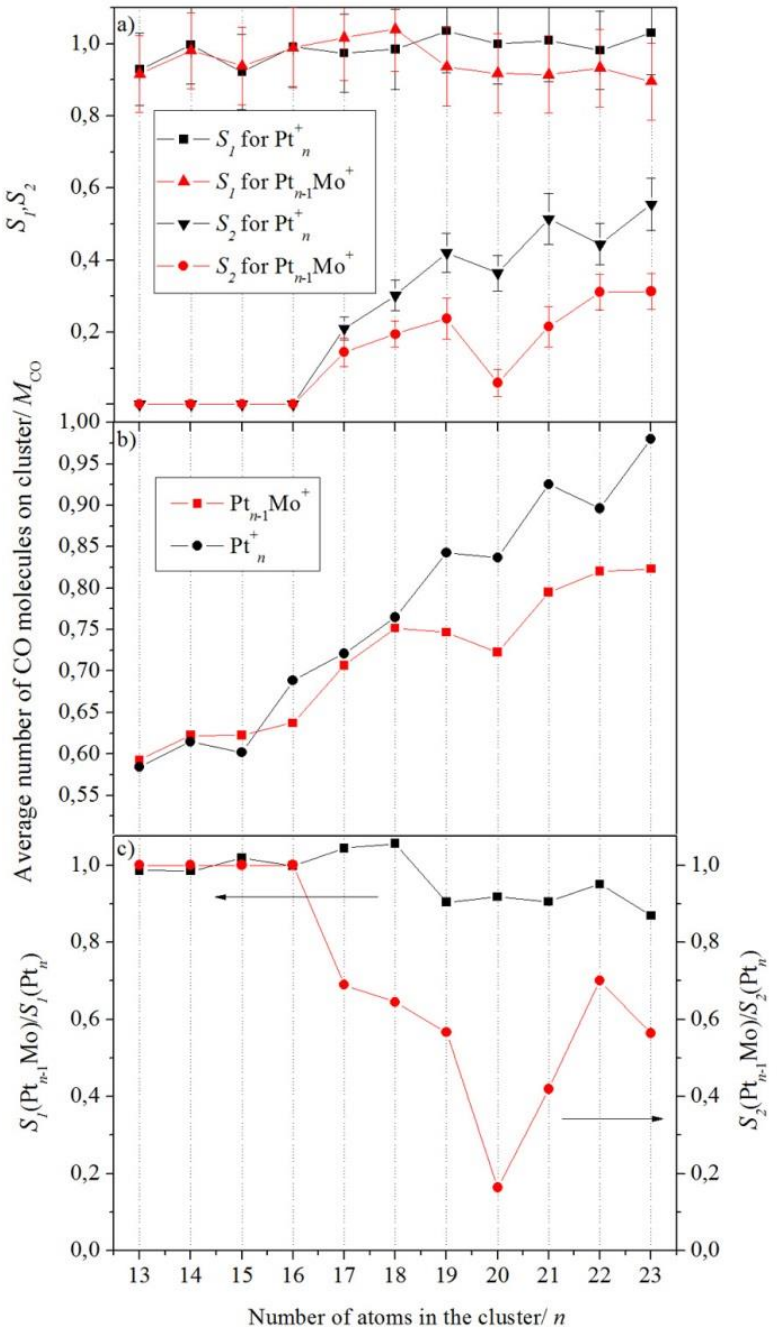
a)
b)
c)
S_1,S_2
S_1 for Pt^+_n
S_1 for $Pt_{n-1}Mo^+$
S_2 for Pt^+_n
S_2 for $Pt_{n-1}Mo^+$
Average number of CO molecules on cluster/ M_{CO}
$Pt_{n-1}Mo^+$
Pt^+_n
$S_1(Pt_{n-1}Mo)/S_1(Pt_n)$
$S_2(Pt_{n-1}Mo)/S_2(Pt_n)$
Number of atoms in the cluster/ n

Fig. 3

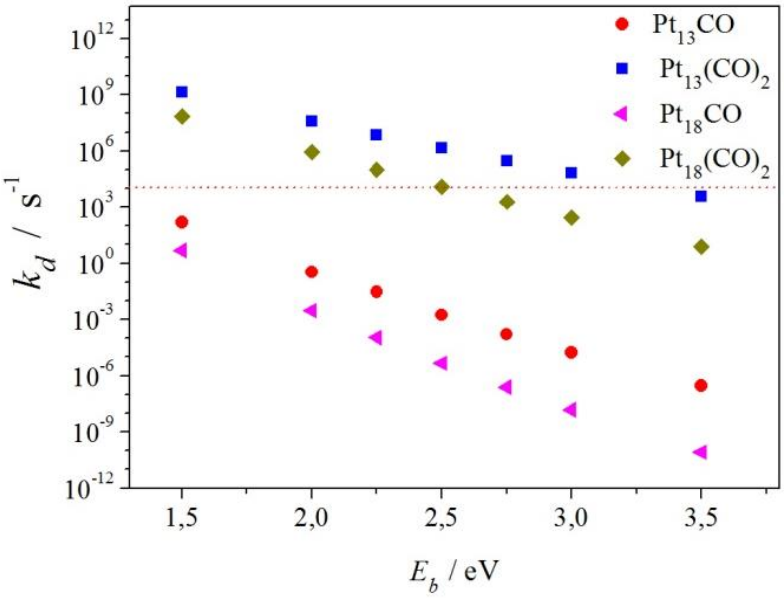
Pt13CO
Pt13(CO)2
Pt18CO
Pt18(CO)2
kd / s-1
Eb / eV
10^12
10^9
10^6
10^3
10^0
10^-3
10^-6
10^-9
10^-12
1,5
2,0
2,5
3,0
3,5

Fig. 4